Congo Sciences
Journal en ligne de l'ACASTI et du CEDESURK
ACASTI and CEDESURK Online Journal
ISSN: 2410-4299, an International Journal

Influence of Working Parameters on the Temperature of Slipper in Hydrostatic Bearings with Circular Pockets of Axial Piston Pump.

WADI TUSAMBILA Valéry *[1], CANBULUT Fazıl[2], UYSAL Ünal[3].

Paper History
Received:
January 13, 2020
Revised:
February 23, 2020
Accepted:
March 05, 2020
Published:
March 27, 2020

Keywords:
Axial piston pump, Slipper Temperature, Working parameters and Lubrication.

ABSTRACT

In axial piston pumps, increasing the temperature of lubricating oil causes undesirable conditions such as degradation of the thermophysical properties of the oil. Among these properties, the viscosity of lubricating oil varies proportionally with the temperature of the oil. Thus, beyond a definite temperature value, the oil no longer fulfills its lubrication function. The consequence is a mixed friction causing an overheating of the slipper, the deformation of the surfaces and finally the wear of the pump. However, temperature of slippers directly affects the lubricating oil temperature. In order to improve energy efficiency and lifetime of piston pump, the present study aims to investigate the influence of operating parameters on the temperature of hydrostatic slipper bearing using a designed experimental set-up. Three different types of slippers were made in bid to observe the effect of slipper geometry on the temperature. This study outcomes show an increasing of the temperature of the slipper with increasing of supply pressure. It has also been found that an increase in the rotation speed induces an increase in the temperature of the slipper. Compared to the slipper- I, with diameter ration De/Di =1.422 and which reaches a temperature of 79°C under a pressure of 30 bar at rotation speed of 300 rpm, the slippers III and II with diameter ratios of 1.784 and 1.69 respectively presented geometries which better minimize the temperature increase of the slippers at 43°C and 47°C respectively under the same conditions.

[1]Département de Génie Mécanique, Faculté Polytechnique, Université de Kinshasa, Kinshasa, R. D. Congo.
[2]Département de Génie Mécanique, Faculté d'ingénierie, Université d'Erciyes, Kayseri, Turquie.
[3]Département de Génie Mécanique, Faculté d'ingénierie, Université de Sakarya, Sakarya, Turquie.
* To whom correspondence should be addressed: ***valerywadi@gmail.com***

INTRODUCTION

In hydraulic systems, the pump plays an important role that of transforming the supplied energy into hydraulic energy. To meet all industrial applications, there are two basic types of pumps: positive displacement and centrifugal. Although axial-flow pumps are frequently classified as a separate type, they have essentially the same operating principles as centrifugal pumps. The piston pump is a rotary unit, which uses the principle of the reciprocating pump to produce fluid flow. Instead of using a single piston, these pumps have many piston-cylinder combinations. A part of the pump mechanism rotates about a drive shaft to generate the reciprocating motions, which draw fluid into each cylinder and then expels it, producing flow. There are two basic types, axial and radial piston; both area available as fixed and variable displacement pumps [AKERS et *al.*, 2006]. Axial piston pump (APP), which is widely used in industrial and construction machinery for converting mechanical power into hydraulic power, is the key component in the hydraulic transmission system. This is due to its high efficiency, power density and structure compactness [TANG et *al.*,2017]. APPs are the main type of engine-driven pumps, whose performance and lifetime are affected by three sliding pairs, specifically the swash plate/slipper pair, cylinder/valve plate pair, and piston/cylinder pair. Compared with other friction pairs of components, slipper pairs are special because they are the direct carrier of the piston cavity pressure, and therefore directly restrict the necessary high speed and high pressure of these pumps [SONG et *al.*, 2018; ELASHMAWY, 2015]. Over the past decades, several numerical, analytical, machine learning and experimental studies on hydrostatic thrust bearing in hydraulic APP have been carried out through considering operating

conditions, geometric parameters and matching materials [BERGADA and WATTON, 2002; Harris et *al.,* 1996; LBOSHI and YAMAGUCHI, 1982; LBOSHI and YAMAGUCHI, 1983]. Many of these studies focused on improving the slipper performance. KOÇ and HOOKE [1996] conducted a theoretical and experimental investigation in order to estimate the effect of clamping ratio, orifice size and three different surface profiles on the performance of slipper. They indicated that the slippers ran satisfactorily with no orifice and had their greatest resistance to tilting couples and to minimum film thickness. WANG and YAMAGUCHI [2002] investigated theoretically and experimentally the characteristics of disk-type hydrostatic thrust bearings supporting concentric loads, simulating the major bearing/seal parts of water hydraulic pumps and motors. They evaluated the characteristics by studying the relationships among the load carrying capacity, pocket pressure, film thickness, and leakage flow rate.

In order to experimentally analyze the effects of slipper geometry and working conditions on the slipper performance, CANBULUT et *al.* [2004] designed an artificial neural predictor used as a predictor for possible experimental applications on modeling bearing system. CANBULUT and SINAOĞLU [2009] designed an experimental set-up to determine the performance of slippers in different conditions. The outcomes of this study revealed that the frictional power loss has been caused by surface roughness, capillary tube diameter and the size of the hydrostatic bearing diameter area, supply pressure and the relative velocity. WANG et *al*. [2015] established and solved the model of friction power loss between slipper and swashplate. Most recently, ÖZMEN et *al*. [2019] used multigene genetic programming and artificial neural network machine learning methods for predicting pressure distribution and leakage behaviour in APP. After comparing performed model results and analytic equations, they reported that artificial neural network results showed better performance than multigene genetic programming and analytic equations. As it can be noticed by analyzing the above-mentioned literature, the performance of slipper friction pairs was studied without taking into account the interactions between temperature and other variables. In circular recessed hydrostatic bearings, the temperature impacts on oil film characteristics are important for analyzing the efficiency of the sliding pairs. The loss of kinetic energy of moving parts due to viscous friction of lubricant causes the reduction of piston pump efficiency. As sliding pairs of axial piston pump moves, both the metal parts and lubricants heat up, which causes temperature to increase significantly, decreases oil viscosity, reduces the bearing capacity of the oil, and intensifies the radial movement of the parts simultaneously. The viscosity of lubricant film is mainly affected by the thermal effect. The shape of the oil film changes, as does the lubrication mode and the trajectory of piston could vary with the changing of oil film [YANG et *al*.,2009]. It is therefore important to assess the temperature variation according to the operating parameters in the bearing material in order to calculate the thermal stresses within slippers. Moreover, this variation is important in the design of slippers because it makes it possible to minimize the increase of the temperature in order to maintain the viscosity of the oil [UYSAL, 1993].

In order to examine the temperature distribution of the slipper in the literature, TURNBULL and SHUTE [1958] examined the influence of temperature on the viscosity and the influence of the slippers shapes on temperature. As a result, a large part of the heat was transmitted to the moving surfaces and another part was thrown out by the oil. Consequently, the energy caused by the viscous drift increased the temperature of the film, thus the viscosity of the oil changed. CAMERON and WOOD [1958] investigated the influence of heat generated in hydrostatic bearings on oil inlet temperature assuming the viscosity does not change. The results showed that the temperature was changing according to the oil film thickness. In addition, they reported that the temperature distribution in the oil film had a parabolic appearance and the maximum temperature was along the line passing through the middle of the oil film. KAZAMA et *al*. [2015] investigated experimentally the relation between Sliding-Part temperature and Clearance Shape of a slipper in swashplate Axial Piston Motor. The experimental setup used in this study comprised a tester, a hydraulic circuit, control units, and measuring instruments. They obtained that the temperature difference distributions of the slipper pad between the maximum and minimum depended on the rotational speed but were independent of supply pressure. Similarly, a hybrid (hydrostatic and hydrodynamic) thrust bearings thermohydrodynamic lubrication model valid for slippers of swashplate type axial piston pumps and

motors was validated by KAZAMA [2018] using experimental results. The comparison of the temperature distributions and center clearances was made at supply pressures up to 35 MPa and rotational speeds up to 26.7 rpm. The simulation showed good agreement with the experiment and the theoretical model was validated. HE-SHENG et *al.* [2016] assessed the influence of thermal effect on hydrostatic slipper bearing capacity of axial piston pump. In order to simplify the calculation process, the effect of hydrodynamic lift characteristic on slipper was not taken into account. The results showed that thermal equilibrium clearance due to solid thermal deformation periodically changes with shaft rotational angle. The slipper bearing capacity increases dramatically with decreasing thermal equilibrium clearance. Recently, in bid to investigate theoretically and experimentally the load-carrying capacity of a slipper pair in an aviation axial-piston pump under specified operating conditions,a thermal hydraulic model based on the lumped parameter method was proposed by HE-SHENG et *al.* [2018]. They noticed that at high oil temperature and high load pressure, while the film thickness decreased with increasing clamping force due to a combined action of the squeezing bearing force and the thermal wedge bearing force, the load-carrying capacity increased.

In order to improve energy efficiency of piston pump, the purpose of the present study is to investigate experimentally the influence of working parameters (supply pressure and rotation speed) on the temperature of hydrostatic slipper bearing.

EXPERIMENTAL ANALYSIS

Theory of the system

Figure 1.a presents a typical swashplate APP. The operating principle is exhaustively explained in CANBULUT and SINANOĞLU [2009]. Swashplate pumps have a rotating cylinder containing pistons. A spring pushes the pistons against a stationary swash plate, which sits at an angle to the cylinder. The slipper carries the load and slide on the slipper plate during the pump operation. For this reason, the slipper must be kept apart from the slipper plate by certain forms of lubrication, otherwise high friction leads to wear and overheating.

Figure 1.b shows a sectioned view of a piston-slipper assembly. The piston itself is shown to be hollow because a lightweight piston is desirable. Both ball- and-

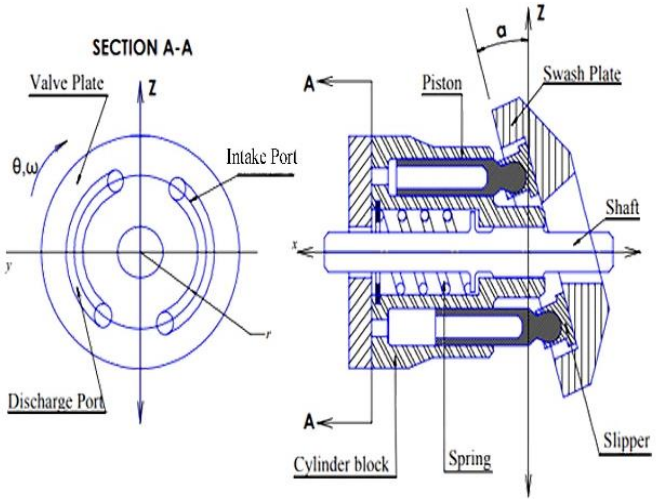

Figure 1.a. General Pump Configuration

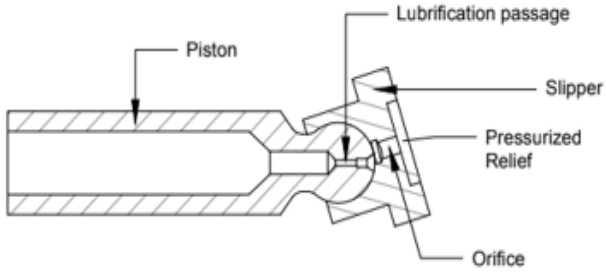

Figure 1.b. Piston / Slipper Geometry

socket joint and swash-plate riding surface are in constant need of oil; therefore, the piston and the slipper are designed with lubrication passages.

Experimental Setup

The schematic diagram of the experimental setup used in the current study for investigating the effect of operating parameters on the temperature of hydrostatic slipper bearing and more details can be found in CANBULUT and SINANOĞLU [2009].

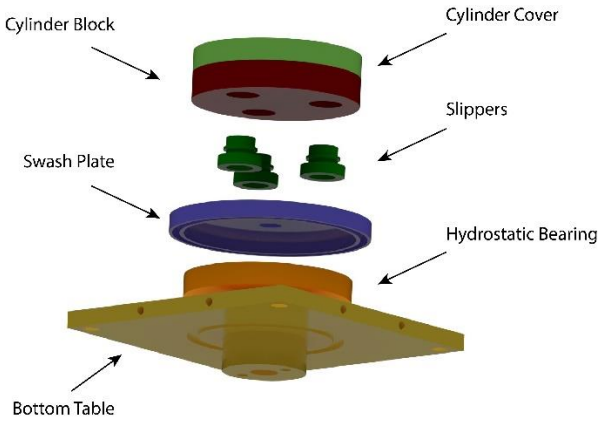

Figure 2. Main test unit

Experimental setup mainly consists of three fundamental units: the main test unit, where the testing of slippers is carried out, the hydraulic power unit, where the power

needed for the experiment is produced, and the driving unit.

As it can be noticed here, the slipper and slipper plate are crucial elements for this study.

The main task of cylinder block is to ensure that the slippers are perpendicular to the turntable and oil pressure delivered to the slipper might be evenly distributed.

As shown in Figure 2, the cylinder block consists of three slippers seats and grooves that provide the pressurized oil to these three slippers. In order to make the slippers suitable for the purpose of the experiments, they were connected to the thermo-couple cables by welding.

Therefore, temperatures were measured from these three zones, namely the hydrodynamic region, the hydrostatic region, and the top surface of the slippers. These zones may be seen in Figure 3. In addition, a manometer was connected to the circular pocket in order to measure the pocket pressure in the hydrostatic region of the slippers.

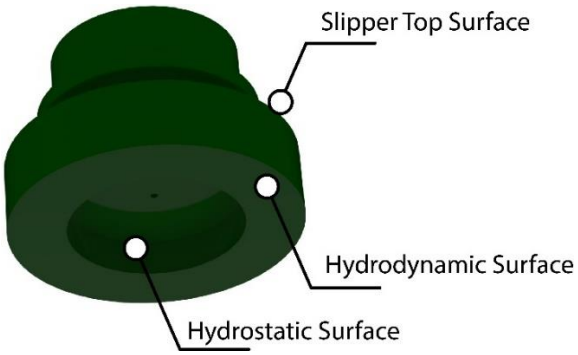

Figure 3. Circular recessed hydrostatic slipper bearing.

The slippers used in the present study were made of brass whose physical properties are presented in Table 1.

Table I. Physical properties of brass

Parameters	Values
Heat transfer coefficient	81 – 116 W/m^{2}K
Specific heat	0.38 kJ/kgK
Density	8600 kg/m^3

Experimental Method

Three types of slippers, named I, II, and III, were used in this study. The outer diameters (De) of all of these slippers were equal to 40mm. The diameter ratios were: De/Di=1.422 for the slipper I, De/Di= 1.65 for the slipper II, and De/Di = 1.784 for the slipper III, where Di is inner diameter. The oil used in the experiment was a commercially available hydraulic oil Shell Tellus S 68, composed of paraffinic base oil and contains high stability, anti-wear, antioxidant and anticorrosive additives. The physical properties of the oil are shown in Table 2.

Table 2: Physical Properties of the oil

Parameters	Values
Density	883 kg/m^3 at 15 °C
Kinematic viscosity	68 mm^2/s at 40 °C
Flash point	222 ^{0}C
Specific heat	1.7165 kJ/kgK
Yield point	-30 ^{0}C

The experiments were carried out at five different pressures (10-20-30-40-50 bar) in each rotation speed (150-300-450-600-750 rpm). Firstly, to circulate oil in experimental setup, a very low-pressure oil (P=1-2 bar) was pumped to the slipper which started to run at a low rotation speed (10 rpm) by using an electric motor. After circulating was completed, thanks to a digital tachometer, speed (150 rpm) and pressure (10 bar) were set. In this way, metal-to-metal contact that may occur in the beginning due to high pressure was prevented in the experiment set. After a period of about 1 minute, hydrodynamic surface, hydrostatic surface, top surface of the slipper, ambient temperature, oil inlet temperature and oil outlet temperatures were respectively read from the digital tachometer. Then, the pressure level was changed from 10 bar to 50 bar by increasing step of 10 bar and the temperatures and flow rates in the aforementioned places were measured. In addition, orifices with three different hole diameters were used for each slipper. When the pressure reached 50 bar and the speed was 750 rpm, the experiments with this slipper and the orifice were completed.

In the experiments, each slipper was equipped with three different orifices (O_1=0.3mm, O_2=0.5mm, O_3=0.7mm) and 225 experiments were performed.

RESULTS AND DISCUSSION

Effects of supply pressure on the temperature of slippers

Figures 4, 5 and 6 show the variation of temperature of slippers with different supply pressures for all the three types of slippers (I, II and III) and three orifices. It can be observed from these figures that temperature of slipper increases, in general, as the pressure increases in the cases of all three slippers. However, it can be noted that when the pressures are higher the increase in temperature of the slipper obtained is less important compared to those recorded while the pressures are lower. In some cases, a drop in temperature is even observed while the pressure increases. This phenomenon can be explained regarding the proportional increase of oil flow with the rise of pressure. As indicated by CANBULUT et *al*. [2009], the inertia forces on the flow are effective with increasing orifice diameter. As the difference between supply pressure and slipper pocket pressure (hydrostatic pressure) increases, oil leakage also increases.

Accordingly, increasing the oil flow augments the quantity of oil in the slipper, thus the quantity of oil in contact with the surface goes up and therefore, attempting to lubricate most of the surface of the slipper.

Slipper- I

The influence of the supply pressure on the temperature of slipper- I is shown in Figure 4 (a-f). For the Orifice O_1 and hydrodynamic surface (Figure 4.a), with a rotation speed of 450 rpm, the increase in temperature observed between the pressures of 10 and 20 bar is about 8^0C whereas between 40 and 50 bar, it is about 2^0C. Similarly, a temperature difference of approximately 16^0C is observed between the pressures of 10 and 20 bars when the speed of rotation is 150 rpm. As mentionned above, the principal cause of this difference could be explained by proportional increase of oil flow with the rise of pressure. At this same rotation speed (150 rpm), a drop in temperature is observed between 40 and 50 bar in the case of the orifice O_2, on the hydrostatic surface of the slipper (Figure 4.d). This could be attributed to the fact that since the orifice O_2 has a greater diameter than the orifice O_1, the amount of oil passing through this orifice to lubricate the slipper will also be greater. It is therefore obvious that the temperature distribution observed in the case of orifice O_2 may be less than that of O_1. With a rotational speed of 600 rpm, on the hydrodynamic surface of the slipper with orifice O_3, the temperature increases from 53 ^{0}C to 74 ^{0}C and decreases when a pressure of 40 bars is reached (Figure 4.e). Contrary to the case of orifice O_1 for which a general ascending trend in temperature is observed, in the case of the slippers endowed with the orifices O_2 and O_3, the analysis of curves shows that the temperature rises normally with pressure, but a sudden drop in temperature is reported from the pressures of 30 and 40 bars respectively for the two hydradynamic and hydrostatic surfaces. This drop in temperature is more accentuated for the higher rotational speeds than the lower ones. Figure 4 also reveals that the highest temperature recorded in the case of slipper- I is 85.5 ^{0} C. It is reached at a pressure and a rotation speed of 40 bars and 750 rpm respectively.

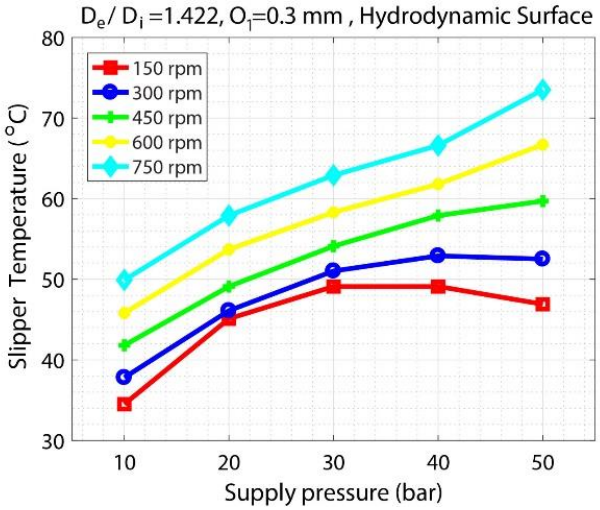

a)

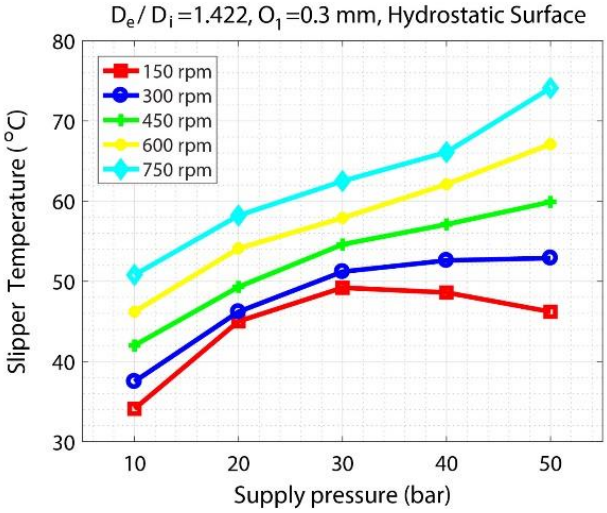

b)

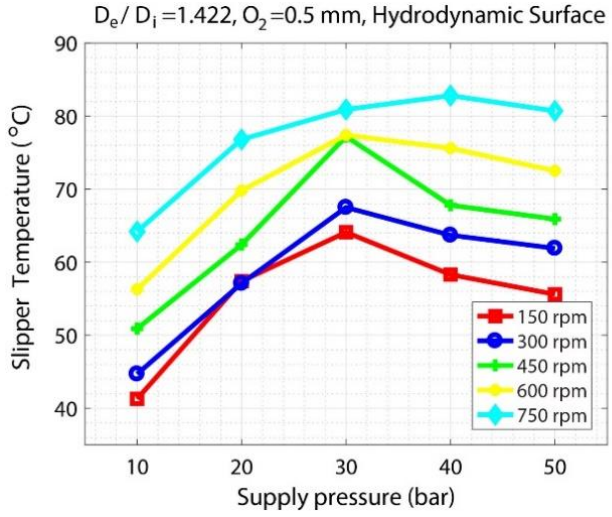

c)

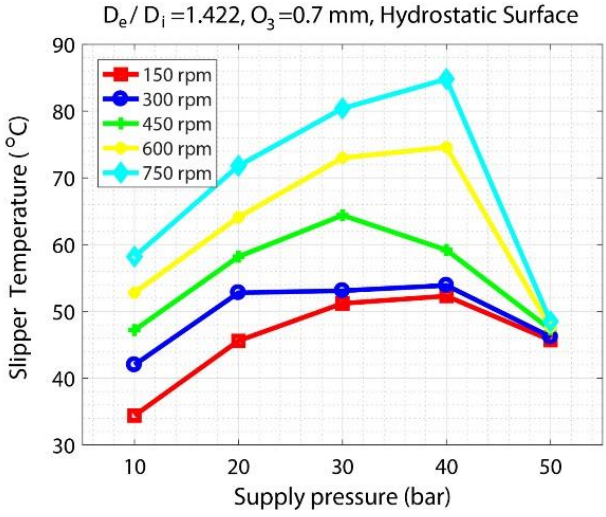

f)

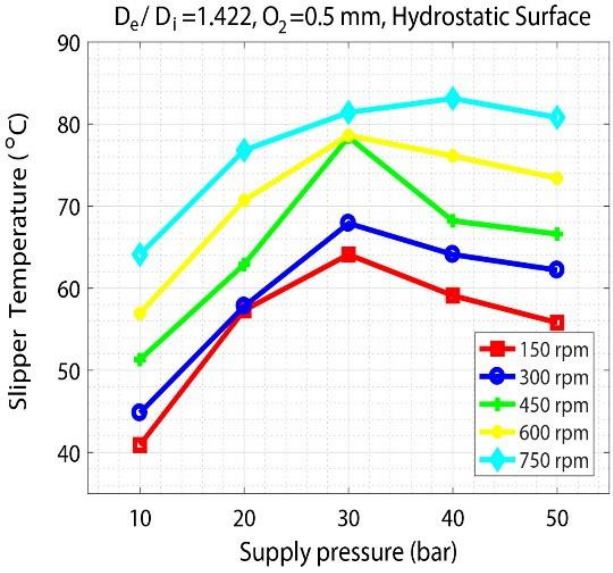

d)

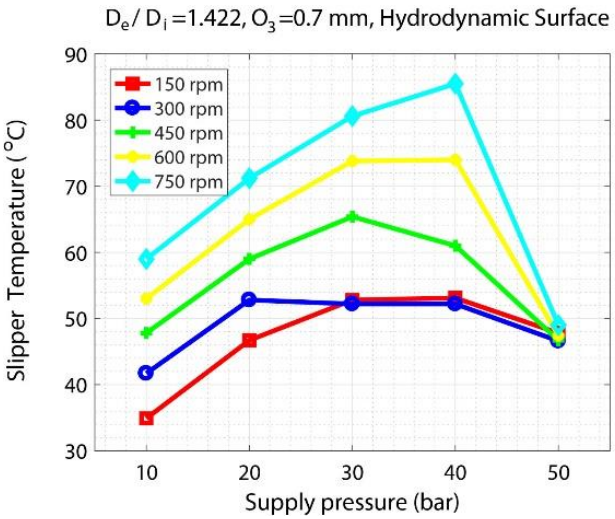

e)

Figure 4. Variation of temperature of slipper- I with different supply pressures.

Slipper- II

Figure 5 (a-f) presents the effect of supply pressure on the temperature of slipper- II. With a rotation speed of 150 rpm, the increase in temperature observed between the pressures of 10 and 20 bar is about 6^0C whereas between the pressures of 40 and 50 bar, it is about 1^0C in the case of orifice O_2 and the hydrostatic surface (Figure 5.d). As shown in Figure 5.b, a temperature difference of about 5^0C is observed between the pressures of 10 and 20 bar when the speed of rotation is 300 rpm whereas temperature difference of about 2^0C is noticed between 40 and 50 bar in the case of the orifice O_3, on the hydrodynamic surface of the slipper. Compared to the temperature of the slipper- I with the supply pressure, it can be observed from the Figure 5 that there is a linear increase in temperature and no sudden and remarkable decrease is recorded. It also can be seen that the highest temperature recorded in the case of slipper-II is about 60^0 C, reached at a pressure and a rotation speed of 50 bars and 750 rpm respectively suggesting a minimization of the temperature better than that of the slipper -I.

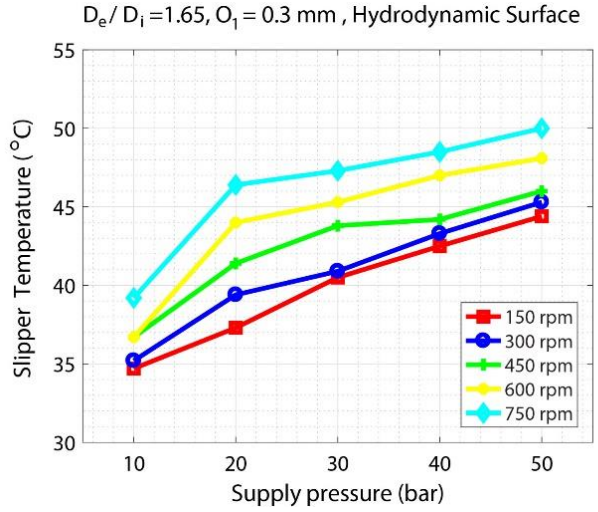

a)

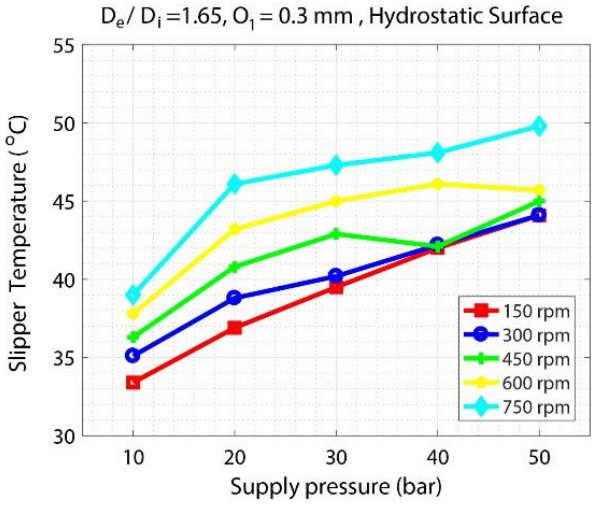

b)

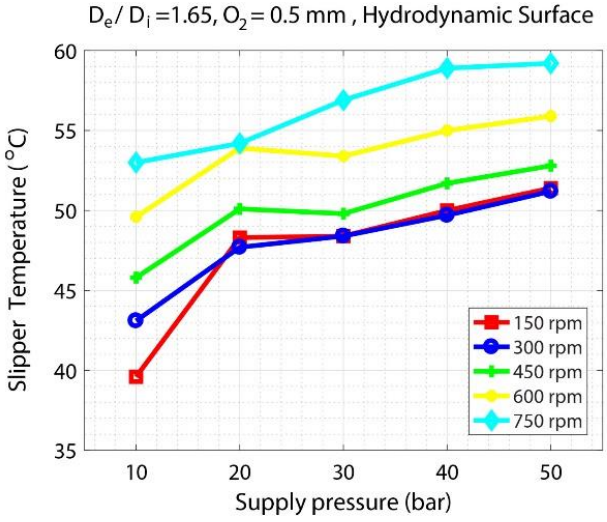

c)

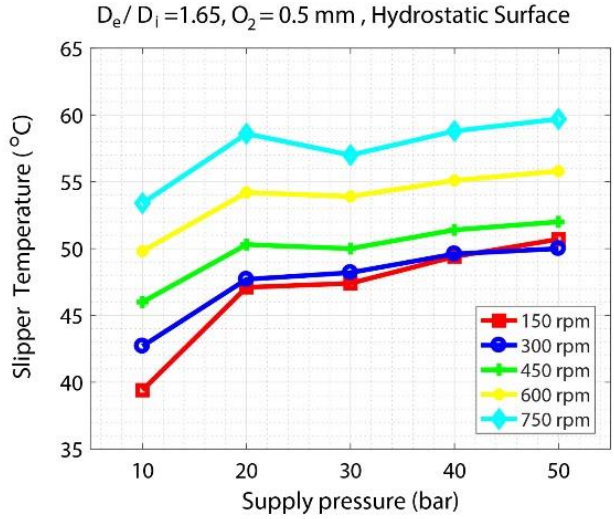

d)

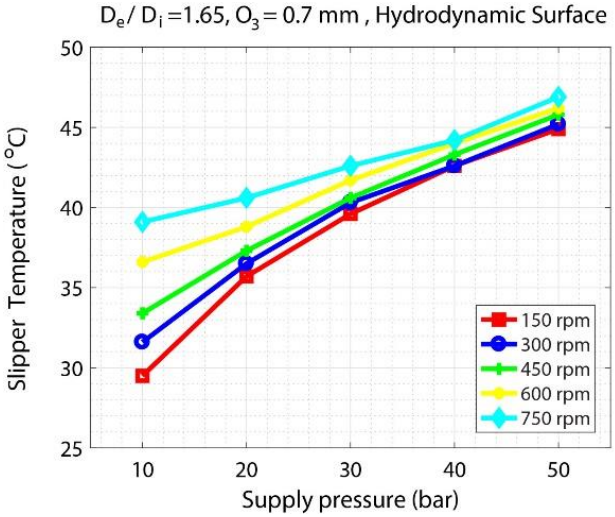

e)

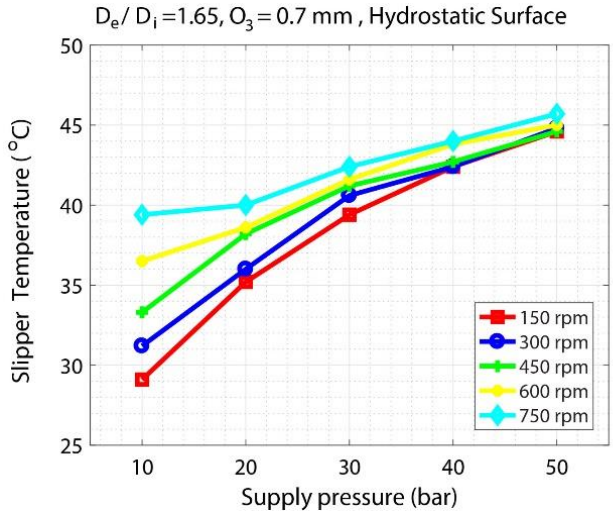

f)

Figure 5. Variation of temperature of slipper- II with different supply pressures

Slipper- III

Figure 6 (a-f) illustrates the variation of temperature of slippers with different supply pressures for slipper-III. The analysis of the figue reveals that, for a

rotation speed of 300 rpm and in the case of the orifice O_1 for example, the increase in temperature observed between the pressures of 10 and 20 bars is about 5^0C whereas between the pressures of 40 and 50 bar, it is about 2^0C. It also can be noticed that for the cases of orifices O_1 and O_3, the temperature of the slipper suggests linear curves and no drop in temperature is observed, which is not the case in the orifice O_2 for which there is a low temperature drop from the pressure of 30 bars. As for the slippers I and II, the temperatures measured from hydrostatic surfaces for the slipper -III seem to be very close to those achieved for the hydrodynamic surfaces. It is very important to indicate that the highest temperature recorded in the case of slipper III is about 50^0 C, obtained at a pressure and a rotation speed of 50 bars and 750 rpm respectively suggesting a minimization of the temperature better than that of the slippers I and II.

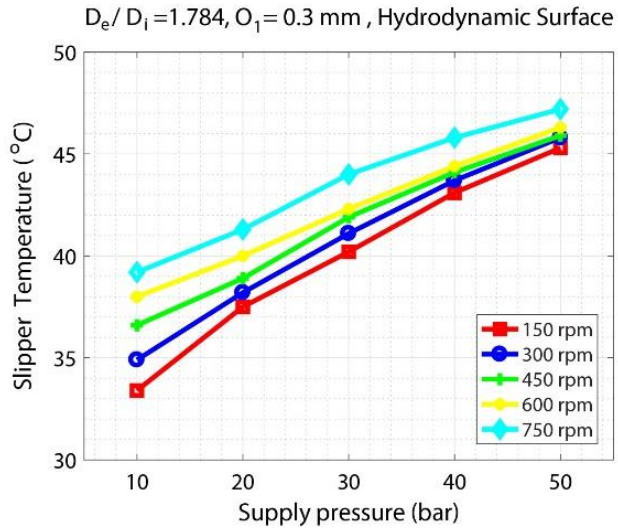

a)

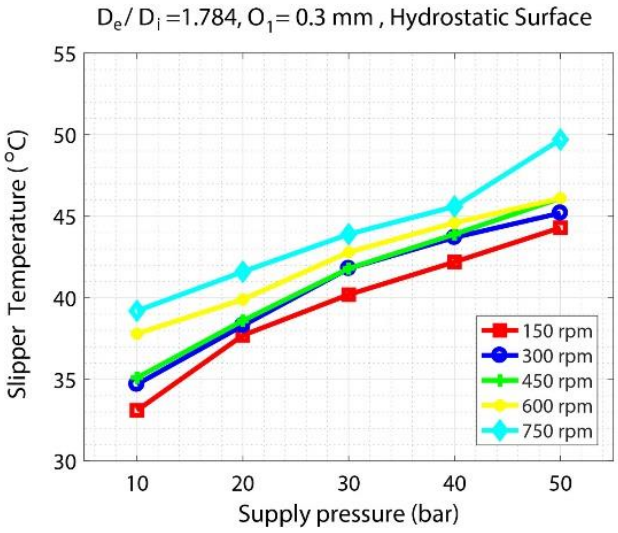

b)

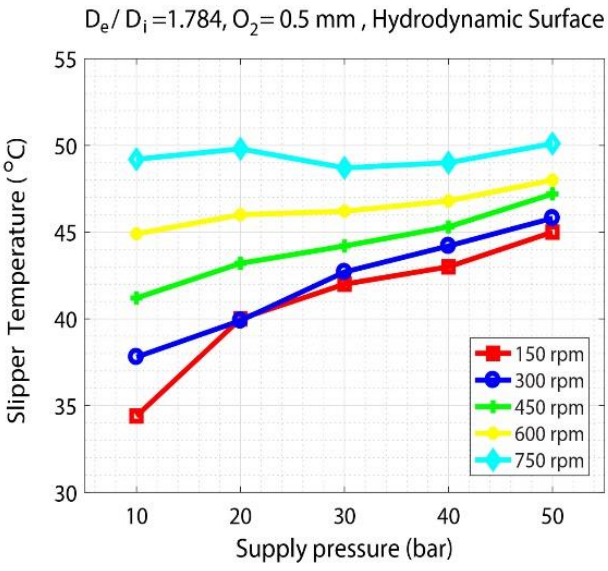

c)

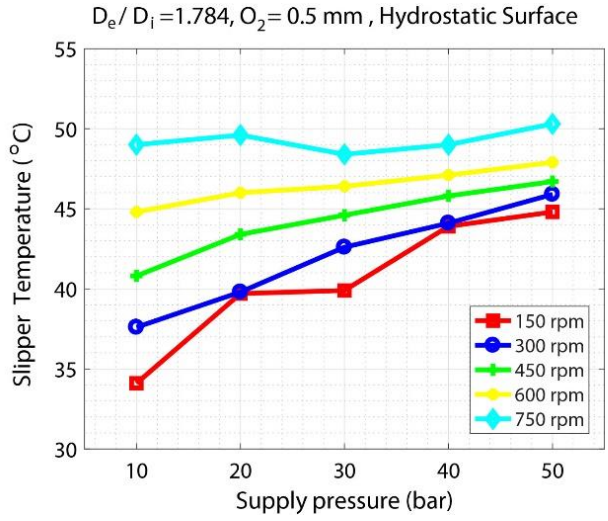

d)

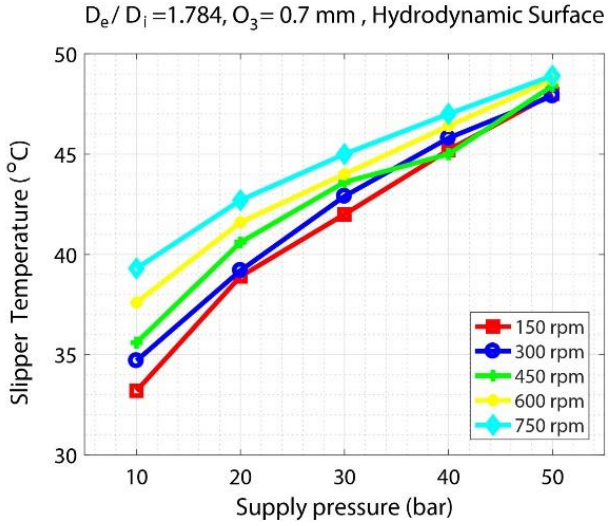

e)

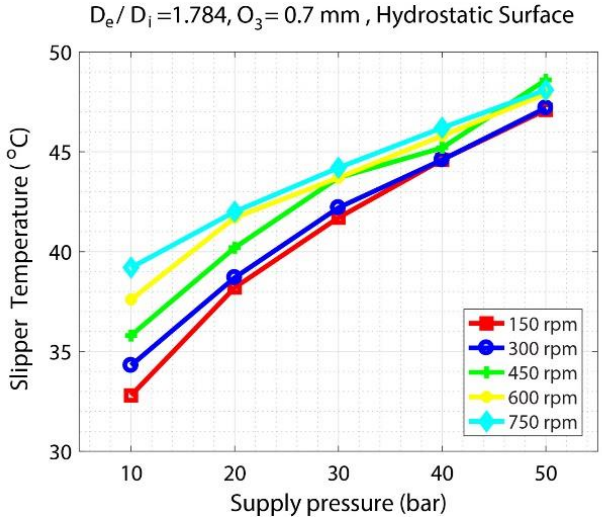

f)

Figure 6. Variation of temperature of slipper- III with different supply pressures.

The maximum temperatures reached for all three slippers (I, II, III) were about 85^{0}C, 60^{0}C and 50^{0}C respectively. This difference can be explained by the geometrical difference of each of the three slippers.

It is also apparent from the analysis of these figures that the temperature distributions recorded for the hydrostatic surfaces of the three slippers are very close to those for the hydrodynamic surfaces.

Effects of rotation speed on the temperature of slippers.

Figure 7 shows the variation of temperature of slippers with different rotation speeds for all the three types of slippers (I,II and III) and three orifices at a constant pressure of 30 bars as average value.

It is clear that an increase in the rotation speed leads to an increase in the temperature of the slipper. When the rotation speed is high, the temperature of the oil increases. As in the case of pressure, the increase in temperature observed is greater in the case of slipper I. This might be attributable to the fact that the slipper is the one with the smallest circular pocket compared to the other two. Therefore, this pocket receives the smallest amount of oil compared to the other two. This same geometrical difference justifies the fact that the temperature observed on the slipper II is higher than that of the slipper III. The maximum temperatures reached for all three slippers (I, II, III) were about 80 ^{0}C, 57 ^{0}C and 48 ^{0}C respectively. This difference can be explained by the geometrical difference of each of the three slippers. Moreover, it can be noticed that in the case of the three slippers, the temperature variations are almost the same for the hydrostatic and hydrodynamic surfaces.

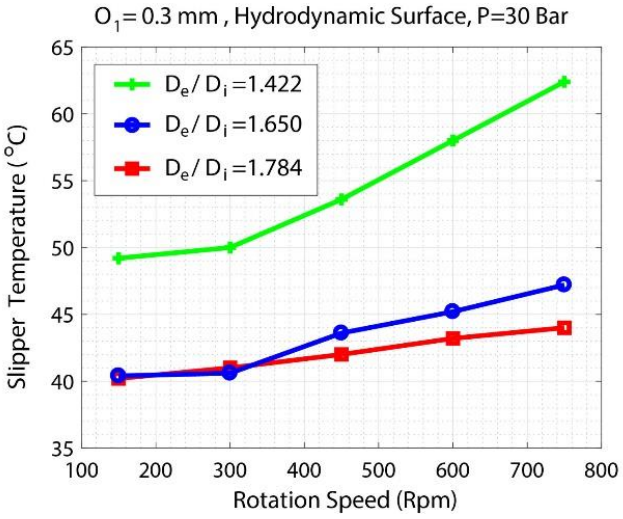

a)

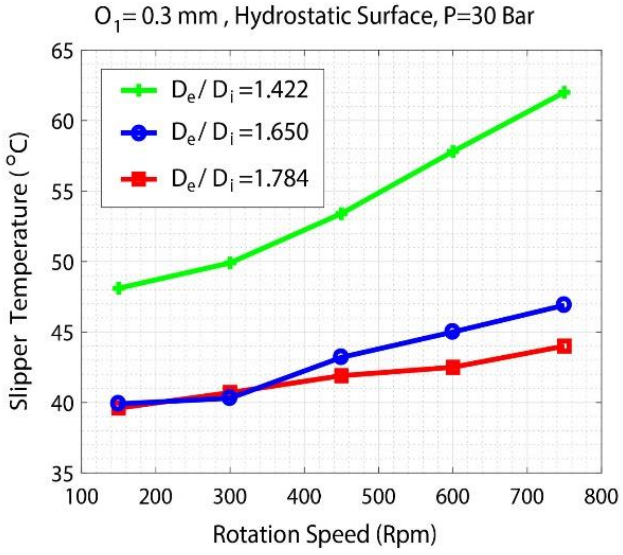

b)

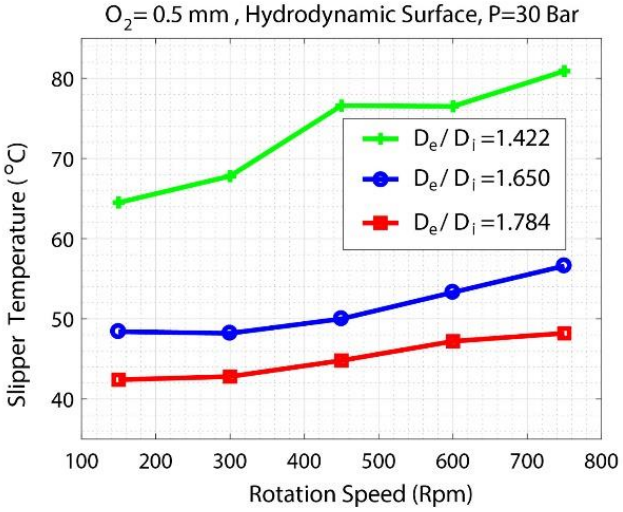

c)

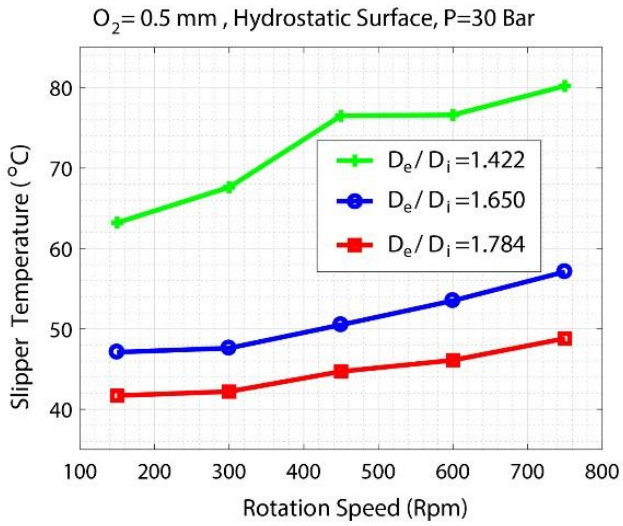

d)

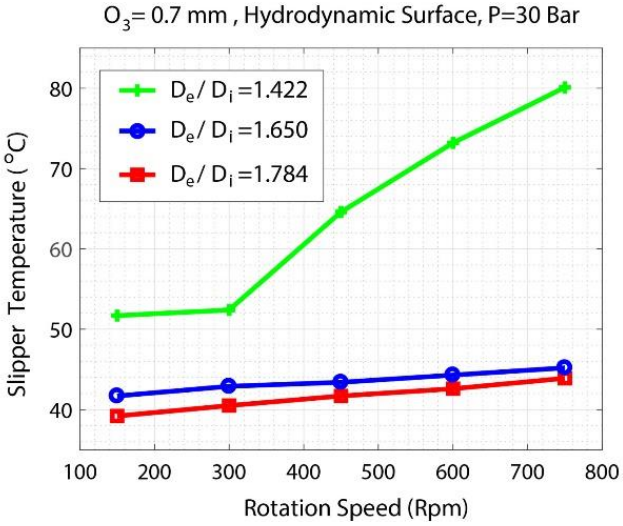

e)

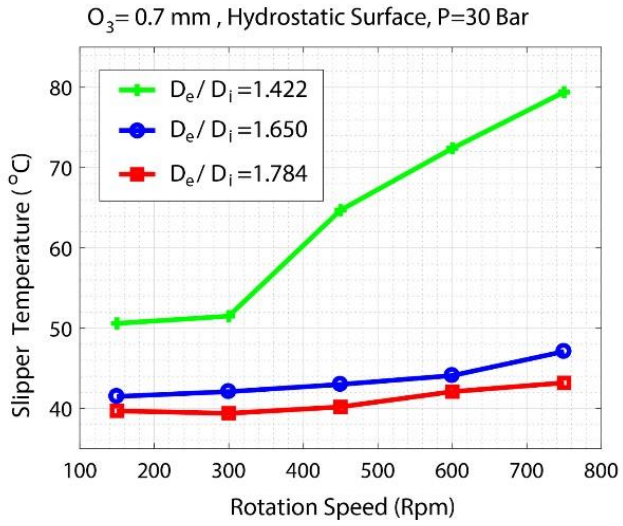

f)

Figure 7. Variation of temperature of slippers with different rotation speeds.

As expected, experimental results from the current study for all three types of slippers are compatible, in general, with the results in the literature. KAZAMA et *al*. [2015] found also the same trend, that of increasing in temperature with the increase of supply pressure and rotation speed.

CONCLUSION

The influence of operating parameters on the temperature of slipper bearing with circular pockets of axial piston pump was experimentally investigated in this study.

The experiments were carried out at five different pressures (10-20-30-40-50 bar) in each rotation speed (150-300-450-600-750 rpm). Three types of slippers made of brass equipped with three different orifices were used.

Based on the achieved test results, the temperature of the slipper increases, in general, with increasing pressure. Moreover, It has been noticed that when the pressures are higher, the increase of the temperature of the slipper obtained is less important compared to that found while the pressures are lower. In some cases, a drop in temperature is even observed as the pressure increases. This phenomenon can be explained on the fact that, mostly the increase of the pressure causes the increase of the flow of oil.

It is clear that an increase in the rotation speed causes an increase in the temperature of the slipper.

In order to compare and validate this experimental study two mathematical and numerical models are envisaged in our future studies. Furthermore, it appears a clear influence of the geometry of the slippers on the temperature of the slippers bearings. Further testing is required to examine this influence, such as determination of the effects of slipper geometry on its temperature.

RESUME

Influence des parametres de fonctionnement sur la temperature du patin dans les paliers hydrostatiques à poches circulaires de la pompe à pistons axiaux.

Dans la pompe à pistons axiaux, l'augmentation de la température de l'huile de lubrification provoque des conditions indésirables telles que la dégradation des propriétés thermo physiques de l'huile.

Parmi ces propriétés, la viscosité de l'huile lubrifiante varie proportionnellement avec sa température. Ainsi, au-delà d'une valeur de température définie, l'huile ne remplit plus sa fonction de lubrification.

La conséquence est un frottement mixte provoquant une surchauffe du patin, la déformation des surfaces et finalement l'usure de la pompe. Cependant, la température du patin affecte directement la température de l'huile de lubrification. Afin d'améliorer l'efficacité énergétique et la durée de vie de la pompe à piston, le présent travail étudie l'influence des paramètres de fonctionnement sur la température du palier hydrostatique à l'aide d'un système expérimental conçu à cet effet. Trois différents types de patins ont été fabriqués pour observer l'effet de la géométrie du patin sur sa température. Les résultats de cette étude revèlent une augmentation de la température du patin avec une augmentation de la pression d'alimentation. Il a également été constaté qu'une augmentation de la vitesse de rotation induit une augmentation de la température du patin. Par rapport au patin I, de rapport de diamètres De/Di=1.422 et atteignant une température de 79^{0}C sous une pression de 30 bars à une vitesse de rotation de 300 tr/min, les patins III et II ayant respectivement des rapports de diamètres de 1.784 et 1.69 ont présenté des géométries qui minimisent mieux l'augmentation de la température à 43^0 C et 47^0 C respectivement dans les mêmes conditions.

Mots Clés

Pompe à pistons axiaux, température du patin, paramètres de fonctionnement et lubrification.

FUNDING

This research did not receive any specific grant from funding agencies in the public, commercial, or not-for-profit sectors.

WARNING

The authors decline all responsibilities for using any information from this study for other purposes than the current one.

REFERENCES

AKERS A., GASSMAN M., SMITH R. [2006]. Hydraulic Power System Analysis. Taylor & Francis Group, LLC, CRC Press, pp. 209-215, New York.

BERGADA J. M., WATTON J. [2002]. Axial Piston Pump Slipper Balance with Multiple Lands, ASME International Mechanical Engineering Congress and Exposition. IMECE 2002. New Orleans Louisiana November 17-22, 2, Paper No. 39338.

CAMERON A., WOOD W.L. [1958]. Parallel surface thrust bearing. Asle Trans. 1 (2) 256.

CANBULUT F., KOÇ E., SINANOGLU C. [2009]. Design of artificial neural networks for slipper analysis of axial piston pumps. Industrial lubrication and Tribology. 61/ 2, 67-77.

CANBULUT F., SINANOĞLU C. [2009]. Experimental Analysis of frictional power loss of hydrostatic sipper bearings. Industrial Lubrication and Tribology.61/3, 123-131.

CANBULUT F., YILDIRIM Ş., SINANOĞLU C. [2004]. Design of an Aıtificial Neural Network for Analysis of Frictional Power Loss of Hydrostatic Slipper Bearings, Tribology Letters, 17,1100-887.

ELASHMAWY M. [2015]. Design of swashplate axial piston machines having low piston transverse forces. International Journal of Mechanical Engineering and Applications.,3(1-2),17-23.

HARRIS R. M., EDGE K. A., TILLEY D. G. [1996]. Predicting the Behavior of Slipper Pads in Swashplate-Type Axial Piston Pumps, Journal of Dynamic Systems, Measurement and Control, Transactions of American Society of Mechanical Engineers. 118,1, 4147.

HE-SHENG T. A. N. G., YAO-BAO Y. I. N., YAN R. E. N., XIANG J., JUN C. H. E. N. [2018]. Impact of the thermal effect on the load-carrying capacity of a slipper pair for an aviation axial-piston pump. Chinese Journal of Aeronautics, 31,2, 395-409.

HE-SHENG T., YAO-BAO Y., YANG Z., JING L. [2016]. Parametric analysis of thermal effect on hydrostatic slipper bearing capacity of axial piston pump. J. Cent. South Univ. 23, 333−343.

IBOSHI N., YAMAGUCHI A. [1982]. Characteristics of a Slipper Bearing for Swash Plate Type Axial Piston Pumps and Motors, Theoretical Analysis, Bulletin of the JSME. 25,210,192l-1930.

IBOSHI N., YAMAGUCHI A. [1983]. Characteristics of a Slipper Bearing for Swash Plate Type Axial Piston Puınps and Motors, Experimental. Bulletin of the JSME. 26,219,1583-1589.

KAZAMA T. [2018]. Thermohydrodynamic lubrication model of a slipper in swashplate type axial piston machines-validation through experimental data. International Journal of Hydromechatronics, 1,3, 259-271.

KAZAMA T., SUZUKI M., SUZUKI K. [2015]. Relation between Sliding-Part Temperature and Clearance Shape of a Slipper in Swashplate Axial Piston Motor. JFPS International Journal of Fluid Power System 8-1, 10-17.

KOÇ E., HOOKE C. J. [1996]. Investigation into the Effects of Orifice Size, Offset and Oveclamp Ratio on the Lubrication of Slipper Bearings. Tribology Intemational, 29(4), 299-305.

ÖZMEN Ö., SINANOĞLU C., BATBAT T., GÜVEN A. [2019]. Prediction of Slipper Pressure Distribution and Leakage Behaviour in Axial Piston Pumps Using ANN and MGGP. Mathematical Problems in Engineering, 2019.

SONG Y., MA J., ZENG S. [2018]. A Numerical Study on Influence of Temperature on Lubricant Film Characteristics of the Piston/Cylinder Interface in Axial Piston Pumps. Energies, 11, 1842.

TANG H., REN Y., XIANG J. [2017]. A novel model for predicting thermoelastohydrodynamic lubrication characteristics of slipper pair in axial piston pump. International Journal of Mechanical sciences. 124-125,109-121.

TURNBULL D. E., SHUTE N. A. [1958]. A preliminary investigation of the characteristics of hydrostatic slipper bearings. British Hydromechanics Research Association, Report RR610.

UYSAL Ü. [1993]. Dairesel Cepli Hidrostatik Yataklarda kayma yüzeyndeki sıcaklık dağılımının Teorik ve deneysel incelenmesi, Master Tezi, Erciyes Üniversitesi, Türkiye.

WANG X., YAMAGUCHI A. [2002]. Characteristics of hydrostatic bearing/seal parts for water hydraulic pumps and motors. Part 1: Experiment and theory [J]. Tribology International. 35,7, 425–433.

WANG Z. B., JIANG H. J., SU Y. [2015]. Power Loss of Slipper within Axial Piston Pump. Applied Mechanics and Materials. 779, 3-12.

YANG H.Y., DING F., YANG X.P., LU Q. [2009]. Hydraulic power systems for trunk line aircrafts. China Mech. Eng. 18, 2152–2159.